Recent Results on the Spatially Resolved Molecular Gas Star Formation Law from CARMA Survey Toward Infrared-bright Nearby Galaxies (STING)

Nurur Rahman[1,†], Alberto D. Bolatto[2], and the STING[‡] Collaboration

[1]Department of Physics, University of Johannesburg, Auckland Park Campus, Johannesburg 2006, South Africa.
[2]Department of Astronomy, University of Maryland, College Park, MD, USA.
†South Africa SKA Fellow.
‡The STING is a collaboration of radio astronomers from USA, Canada, Germany, and South Africa.

E-mail: nrahman@uj.ac.za; nurur@yahoo.com

Abstract. The functional relationship between star formation rate surface density and molecular gas surface density in galaxies is commonly known as the star formation law. Observational determinations of this law require taking into account a number of factors. The extinction, contributions from non star-forming populations affect many measures of star formation, the treatment of the diffuse emission, and the statistical methodologies employed all have impacts on the precise relation between gas and star formation. Using CARMA STING data-set, a 3mm (CO J = 1-0) survey of nearby galaxies, we recently investigate the relationship at the sub-kpc level.

We find that the precise observational constraint on the linear or non-linear functional form of the relationship requires an accurate estimate of the fraction of the diffuse emission. Our results show that the treatment of the diffuse emission has significant impact on the intrinsic scatter in the Schmidt-Kennicutt type star formation law. The scatter varies substantially with the choice of the star formation tracer used. For example, the mid-infrared non-linear 24 μm star formation tracer shows the tightest correlation with the molecular gas content whereas (azimuthally averaged) extinction corrected Hα as a star formation tracer appears to be the noisiest. By measuring the relationship in the bright, high molecular gas surface density ($\Sigma_{\rm H_2}\sim$20 M$_\odot$ pc^{-2}) regions of the disks to minimize the contribution from diffuse extended emission and using 24 μm emission as a tracer of star formation, we find an approximately linear relation between molecular gas and star formation rate surface density with a molecular gas depletion time $\sim$2.30 Gyr.

1. Introduction

Stars form within molecular clouds. However, the processes responsible for converting molecular gas into stars in various galactic environments are still poorly understood. Observations find that the star formation rate (SFR) and the gas content in galaxies are related by, $\Sigma_{\rm SFR} = {\rm A}\ \Sigma^{\rm N}_{\rm gas}$, where $\Sigma_{\rm SFR}$ and $\Sigma_{\rm gas}$ are the star formation rate surface density and the gas (atomic and molecular) surface density, respectively; and A is the normalization constant representing the

efficiency of the processes ([1], [2], [3], [4], [5]). This relationship between gas and SFR surface densities is commonly referred to as the Schmidt-Kennicutt star formation (SF) law.

Spatially resolved SF law studies, whether it is a rigorous case study or a meticulous investigation of a sample, frequently reach dissimilar conclusions on the value of the exponent in the relation above when relating *molecular gas* to SFR (hereafter we express the exponent as N_{mol} to represent the molecular gas SF law). These studies provide a spread in the value of the power law index ranging from $N_{mol} \sim 0.8 - 1.5$ ([6], [7], and references therein). Whether the local SF law is linear or non-linear has implications for the dominant SF mechanisms as well as for modeling efforts. The range in the index of the SF law observed within and among galaxies may be intrinsic and contain valuable astrophysical information, or be entirely attributable to the different choices of gas and SFR tracers, methodologies for internal extinction correction, differences in the CO-to-H_2 conversion, or the range of spatial scales probed.

To explore the impact of various methodological aspects related to the local SF law we recently make two comprehensive analyses of the SF law using high resolution ($3'' - 5''$) STING[1] CO $J = 1 - 0$ data procured from Combined Array for Research in Millimeter Astronomy (CARMA) interferometer observations. Our results are presented in [6] and [7]. Rahman *et al* 2011 [6] is a pilot project which centers on 1) the use of different SFR tracers and the scatter associated with those tracers, 2) the role of the diffuse emission (DE), a component of the integrated disk emission which is not necessarily related to the star-forming regions, and 3) the role of fitting methodologies and data sampling strategies in determining the functional form of the SF law. The insights obtain from this work leads us to further investigate the local SF at high (molecular gas) surface brightness regions for the STING sample galaxies [7]. In this report we underline the key results obtained from these studies.

2. Data

The sample is composed of 23 northern ($\delta > -20°$), moderately inclined ($i < 75°$), and nearby galaxies (within 45 Mpc) which are taken from the *IRAS* Revised Bright Galaxy Survey (RBGS; [8]). These galaxies have been carefully selected to have uniform coverage in stellar mass ($\sim 10^{8.1} - 10^{11.5}$ $M_\odot$), SF activities ($\sim 0.05 - 12.30$ $M_\odot$ Gyr^{-1} pc^{-2}), and morphological types.

We use CO $J = 1 - 0$ spectral cube to produce integrated CO intensity maps. We apply a conversion factor, $X_{CO} = 2.0 \times 10^{20}$ $cm^2/(K\ km\ s^{-1})$, to convert intensity maps to molecular gas column density maps. To construct SFR tracer maps for the sample we use 24 μm images from the Multi-band Imaging Photometers (MIPS; [9]) instrument on board the *Spitzer Space Telescope*. The calibrated mid-infrared images are obtained from the *Spitzer* Heritage Archive. The FUV and Hα images of NGC 4254 are obtained from *GALEX* Nearby Galaxies Survey [10] and *Spitzer* Infrared Nearby Galaxies Survey [11]. The spatial resolution of our studies is limited by the point spread function of the 24 μm map, which has a FWHM of $6''$. This angular resolution covers a range of physical scales in the sample ($\sim$160-1250 pc) for varying physical distances of individual galaxies ($\sim$5.5-43.1 Mpc). Higher resolution images were Gaussian-convolved to have the same image resolution and pixel sampling.

Construction of various data products such as molecular gas surface density (Σ_{H_2}) map, SFR surface density (Σ_{SFR}) map and the associated error maps as well as data sampling and fitting strategies are described in detail in [6]. We use unsharp masking to model and remove the DE from the SFR tracer maps. However, unlike [6] which uses combined CO data (both single dish and interferometer), in this report we use only CARMA data to obtain molecular hydrogen. Since interferometric observation filters out extended emission, the CO data does not warrant the need to remove the DE.

[1] PI: A. D. Bolatto, University of Maryland, MD, USA; http://www.astro.umd.edu/∼bolatto/STING/

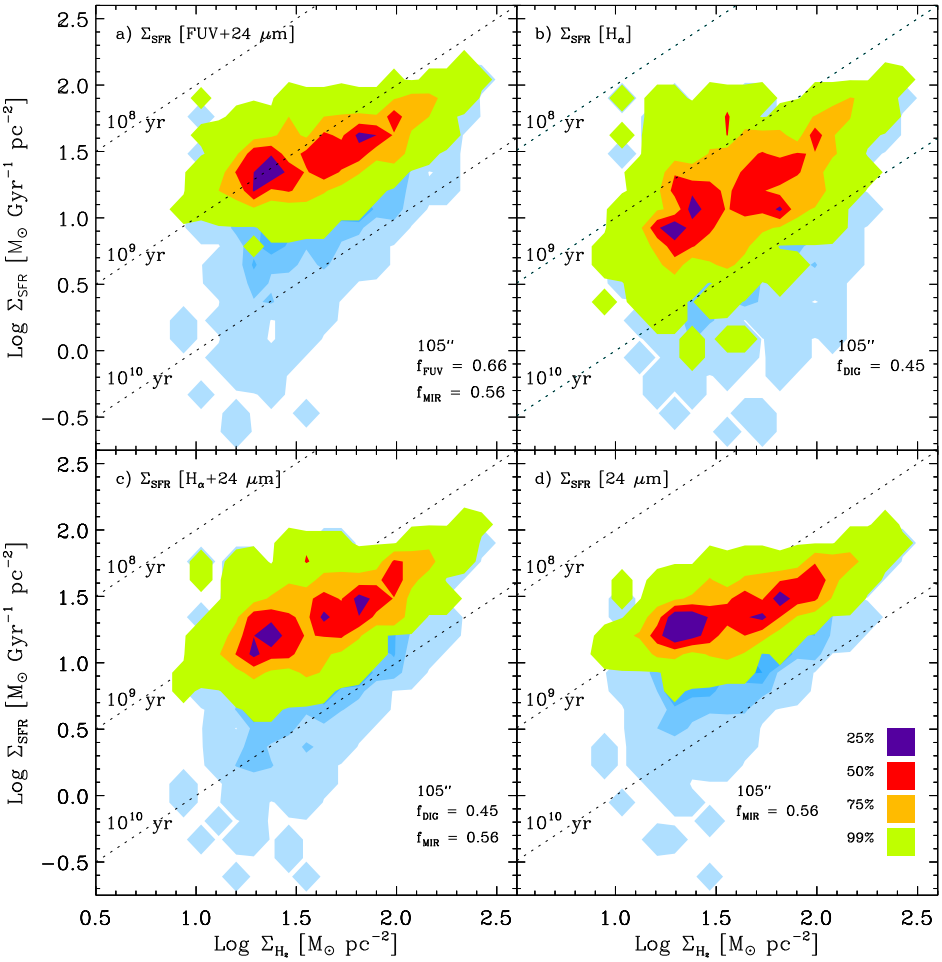

Figure 1. Pixel analysis of the observed $\Sigma_{\rm SFR}$ - $\Sigma_{\rm H_2}$ relationship for NGC 4254 at 6″ resolution using four different SFR tracers (NGC 4254 a STING member galaxy). The figure shows the relationship when no DE is subtracted from the total emission of the SFR tracer (green-brown-red-blue contours) and at one particular filter scale of unsharp masking (blue contours) to highlight the significance of the subtraction of DE in the SF law. The contours are placed at 90%, 75%, 50%, and 25% of the maximum frequency. The diagonal dotted lines represent constant star formation efficiency (ϵ) where ϵ ∼100%, 10%, and 1% correspond to gas depletion time scale, $\tau_{\rm dep}$=0.1, 1.0, and 10 Gyr. The 1σ sensitivity limit of $\Sigma_{\rm H_2}$ map is ∼5.3 $M_\odot$ pc^{-2} which is derived from CARMA CO $J = 1 - 0$ observation. NGC 4254 is a normal star-forming spiral located at a kinematic distance of 16.6 Mpc. The 6″ angular scale corresponds to a physical length of ∼480 pc in the disk of the galaxy. It is apparent that the subtraction of the DE affects the low surface density regions and hence the functional form of the $\Sigma_{\rm SFR}$ - $\Sigma_{\rm H_2}$ relationship. It is also obvious that $\Sigma_{\rm H\alpha}$ shows the largest scatter among all SFR tracers.

3. Results and Analyses

3.1. NGC 4254: A Detailed Case Study

In Rahman *et al* 2011 [6] we exploit multi-wavelength data-set of NGC 4254 to conduct a thorough investigation of the impact of various methodological features in determining the

functional form of the SF law. The available data facilitates a detailed analysis using four different SFR tracer maps including FUV and 24 μm, extinction corrected Hα, observed Hα and 24 μm, and only 24 μm. We construct these maps following the prescriptions provided by [12], [13], and [14]. The variety of indicators is critical in appraising the robustness of the $\Sigma_{\rm SFR}$ - $\Sigma_{\rm H_2}$ relationship against the treatment of the DE. The details of different data samplings, various fitting considerations, and the technique to remove the DE can be found in [6].

Figure 1 underscores the results obtained from the pixel sampling and the OLS bisector fitting method only. In this figure a direct relation between the slope of the SF law and the magnitude of the DE subtracted in the pixel analysis is conspicuous: *subtraction of higher diffuse fraction corresponds to a steeper power-law index*. Compared to other sampling methods, this trend is *only* observed in the pixel analysis which contains the low surface brightness regions. Since the DE is proportionally more important in fainter regions, its subtraction increases scatter in the gas-SFR relation mostly at low surface densities. As a result, removing the DE steepens the SF law. It is also evident that the scatter in the SF law is substantially lower when no DE is subtracted from the total emission of the SFR tracers.

Among all SFR tracers, mid-infrared 24 μm displays the tightest correlation with the molecular gas ($\sigma\sim$0.2 dex from the OLS fitting). This is likely due to a combination of two effects: 1) the times scales for GMC dissipation by massive star formation and 24 μm emission are essentially the same, and 2) by its nature, this SFR tracer does not need to be corrected by extinction. The extinction-corrected $\Sigma_{\rm H\alpha}$ shows the largest scatter ($\sigma\sim$0.5 dex). This bearing is persistent regardless of the level of the unsharp masking applied to remove the DE. This is due to the fact that the extinction correction is azimuthally averaged, and it does a poor job at correcting any one position although it yields the correct result in a statistical sense.

3.2. The Sample

Rahman *et al* 2012 [7] examines $\Sigma_{\rm SFR}$ - $\Sigma_{\rm H_2}$ relation for 14 STING galaxies (including NGC 4254) by setting $\Sigma_{\rm H_2} > 20$ M$_\odot$ pc^{-2}. This threshold is chosen to ensure that: 1) the signal-to-noise is good, 2) interferometric deconvolution issues are minimized, 3) the potential contribution by the DE is less problematic, and 4) we focus on regions dominated by molecular gas. The selection of galaxies is based on secured CO $J = 1 - 0$ detection, availability of data at other wavelengths, and the $\Sigma_{\rm H_2}$ threshold mentioned above. In this subset, the molecular gas and star surface densities span a wide range, $\Sigma_{\rm H_2}\sim$20-1000 M$_\odot$ pc^{-2} and $\Sigma_{\rm SFR}\sim$4-570 M$_\odot$ Gyr^{-1} pc^{-2}. The stellar mass M$_*$ ranges in between $\sim 10^{9.7} - 10^{11.5}$ M$_\odot$.

The left panel of Figure 2 highlights spatially resolved pixel analysis for the STING sample. A simple correlation test shows that the points in this diagram are strongly correlated. We find a Pearson correlation coefficient r$\sim$0.7. The OLS bisector method yields a power-law index N$_{\rm mol}$ $\sim$1.1$\pm$0.1 where the error is derived from bootstrapping. This is an intriguing result. Despite the fact that these measurements are coming from wide variety of galactic environments and galaxy properties, the result suggests that the ensemble of points yields an approximately linear SF law. The right panel of Figure 2 shows molecular gas depletion time as a function of molecular gas surface density. The construction of the means and the error bars did not include the data points from NGC 772 and NGC 3147 (see [7] for detail explanation). It is clear from this diagram that the H_2 depletion time has at most a very weak dependence on $\Sigma_{\rm H_2}$. A small correlation coefficient (r$\sim$0.2) suggests that $\tau_{\rm dep}$ is mostly uniform across the disk.

The uniformity of $\tau_{\rm dep}$ over a wide range of $\Sigma_{\rm H_2}$ is most naturally explained as a consequence of the approximate constancy of the depletion time for molecular gas in GMCs. Indeed the observations of Local Group galaxies suggest that the properties GMCs are fairly uniform ([16], [17], [18]). In this scenario a linear SF law follows naturally, where the $\Sigma_{\rm SFR}$ - $\Sigma_{\rm H_2}$ relation arises from the number of GMCs filling the beam ([14], [15]). A linear molecular gas SF law is consistent with the scenario in which GMCs turn their masses into stars at an approximately

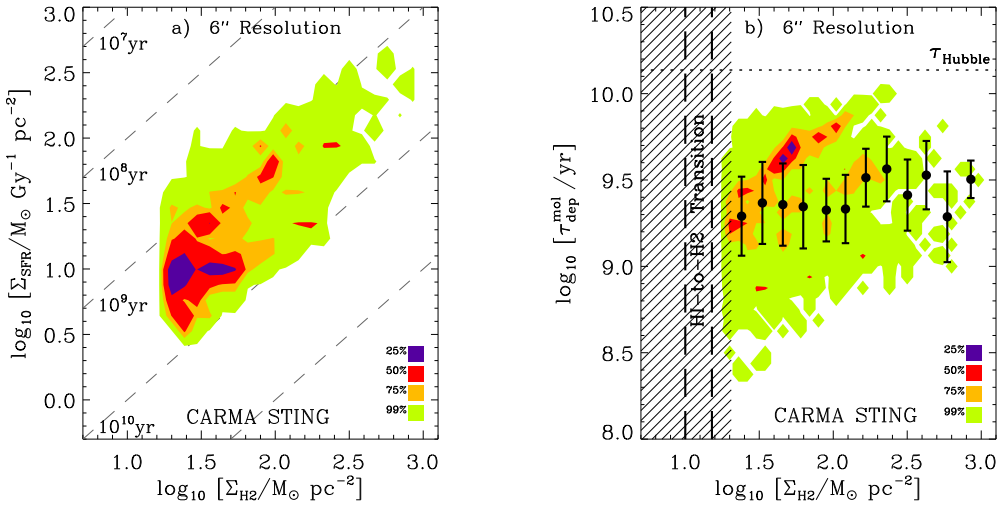

Figure 2. Panel a: Pixel analysis of the observed Σ_{SFR} - Σ_{H_2} relationship at 6″ resolution 14 CARMA STING galaxies (the original sample contains 23 galaxies). The panel shows a smoothed two-dimensional distribution where each point is weighted by the inverse of the total number of points of the contributing galaxy (all galaxies are equally important in the distribution, irrespective of the number of points they contribute). The contours of the smoothed distribution enclose 99%, 75%, 50% and 25% of the total. The diagonal dashed lines represent τ_{dep} as in Fig. 1. **Panel b:** Molecular gas depletion time (τ_{dep}) versus Σ_{H_2} at 6″ resolution for the same galaxies shown in panel a. The horizontal dotted line represents the Hubble time, and the filled circles and associated error bars in black represent the median and 1σ dispersion in Σ_{H_2} bins. The gray hatch illustrates the region where $\Sigma_{H_2} < 20$ M$_\odot$ pc^{-2} which we remove from our analysis. Observational studies suggest that HI-to-H_2 phase transition occurs around Σ_{H_2} ∼10-15 M$_\odot$ pc^{-2} and the nature of the (total) gas-SFR surface density relation changes dramatically around this range [13]. By sampling high Σ_{H_2} regions, $\Sigma_{H_2} > 20$ M$_\odot$ pc^{-2}, we, therefore, investigate the SF law in the molecular region of a galaxy disk [7].

constant rate, irrespective of their environmental parameters [19].

4. Summary and Conclusions

It is important to note that the different choices of SFR tracers and spatial scales mean sampling different SF histories and different time scales in a galaxy. It is also possible that these differences correspond to a spectrum of physical SF mechanisms present in a wide range of environments. Using CARMA STING data-set we analyze the relationship between the SFR and molecular gas surface densities at the sub-kpc level to explore how the functional form of the SF law depends on the treatment of various data sampling. We also critically examine how different fitting techniques influence the outcome. In particular, we probe in-depth the contribution of the DE in various SFR tracers and its consequences on the spatially resolved SF law.

We find that a precise observational constraint on the linear or non-linear functional form of the relationship requires an accurate estimate of the fraction of the DE. Our results show that the treatment of the DE has notable impact on the intrinsic scatter in the canonical SF law. The scatter varies substantially with the choice of the SF tracer used. For example, the non-linear 24 μm star formation tracer shows the tightest correlation with the molecular

gas content whereas (azimuthally averaged) extinction corrected Hα as a tracer appears to be the noisiest. By measuring the relationship in the bright, high molecular gas surface density ($\Sigma_{H_2} \sim$ 20 $M_\odot$ pc^{-2}) regions of the disks to minimize the contribution from diffuse extended emission and using 24 μm emission as a tracer of SF, we find an approximately linear relation between molecular gas and star formation rate surface density with a molecular gas depletion time $\sim$2.30 Gyr.

Acknowledgments
NR acknowledges support from the South Africa Square Kilometer Array (SKA) Postdoctoral Fellowship program. The authors thank SINGS and GALEX NGS teams for their excellent data set. This work has made use of the NASA/IPAC Extragalactic Database (NED) which is operated by the JPL/Caltech, under contract with NASA. Support for CARMA construction was derived from the Gordon and Betty Moore Foundation, the Eileen and Kenneth Norris Foundation, the Caltech Associates, the states of California, Illinois, and Maryland, and the NSF. Funding for ongoing CARMA development and operations are supported by NSF and CARMA partner universities.

5. References

[1] Schmidt M 1959 *ApJ* **129** 243
[2] Schmidt M 1963 *ApJ* **137** 758
[3] Sanduleak N 1969 *AJ* **74** 47
[4] Hartwick F D A 1971 *ApJ* **163** 431
[5] Kennicutt R C Jr 1989 *ApJ* **344** 685
[6] Rahman N, Bolatto A D, Wong T, *et al* 2012 *ApJ* **730** 72
[7] Rahman N, Bolatto A D, Xue R, *et al* 2011 *ApJ* **745** 183
[8] Sanders D B, Mazzarella J M, Kim D C, Surace J A, and Soifer B T 2003 *AJ* **126** 1607
[9] Rieke G H, *et al* 2004 *ApJs* **154** 25
[10] Gil de Paz A, *et al* 2007 *ApJS* **173** 185
[11] Kennicutt R C Jr *et al* 2003 *PASP* **115** 928
[12] Calzetti D, *et al* 2007 *ApJ* **666** 870
[13] Kennicutt R C Jr *et al* 2007 *ApJ* **671** 333
[14] Bigiel F, Leroy, A, Walter F *et al* 2008 *AJ* **136** 2846
[15] Komugi S, Sofue Y, Nakanishi H, Onodera S, and Egusa F 2005 *PASJ* **57** 733
[16] Blitz L, Fukui Y, Kawamura A, *et al* 2007 *ProtoStars and Planets* vol V, ed B Reipurth, D Jewitt, *et al* (Tucson: University of Arizone Press) p 81
[17] Bolatto A D, Leroy A K, Rosolosky E, Walter F and Blitz L 2008, *ApJ* **686** 948
[18] Fukui Y and Kamagura A 2010 *Annu. Rev. Astron. Astrophys.* **48**, 547
[19] Krumholz M R and McKee C F 2005 *ApJ* **630** 250